ISSN 1070-3632, Russian Journal of General Chemistry, 2014, Vol. 84, No. 10, pp. 1877–1887. © Pleiades Publishing, Ltd., 2014.
Original Russian Text © A.G. Davidian, A.G. Kudrev, L.A. Myund, O.S. Khlynova, M.K. Khripun, 2014, published in Zhurnal Obshchei Khimii, 2014, Vol. 84, No. 10, pp. 1596–1606.

Structure of Aqueous Electrolyte Solutions Estimated by Near Infrared Spectroscopy and Chemometric Analysis of Spectral Data

A. G. Davidian, A. G. Kudrev, L. A. Myund, O. S. Khlynova, and M. K. Khripun

St. Petersburg State University, Universitetskii pr. 26, St. Petersburg, 198504 Russia
e-mail: AGDavidian@yandex.ru

Received June 23, 2014

Abstract—The IR spectra of aqueous solutions of $MClO_4$, MNO_3, MCl (M = Li, Na), CsCl, and Na_2SO_4 were measured at frequencies of 5400–7500 cm^{-1} over a wide concentration range from 0.12 M up to saturation concentrations at 25°C. Chemometric analysis of the experimental data matrix was performed. Regularity was detected in distribution of the IR spectra of the studied aqueous solutions on the the plot of analysis scores by the principal component method depending on the nature of the anion–water interaction. The influence of the nature of the salt anion and cation on the water structure in aqueous electrolyte solutions was demonstrated. The existence and interconversion of the spectral forms of water with changing electrolyte concentration in solution were revealed.

Keywords: aqueous solution, NIR spectroscopy, chemometric analysis

DOI: 10.1134/S1070363214100028

The choice of aqueous solutions of lithium and sodium salts for this study was dictated by important role played by these systems in natural physicochemical, physiological, and biological processes, as well as by their wide industrial application.

When introduced into water, an electrolyte is known to cause changes in its physical and physicochemical properties. The processes and structural changes in dilute solutions are described by the Frank–Wen model [1] which assigns the dominant role to liquid water. In passing to concentrated solutions, this approach becomes inapplicable, since any considerations on the intrinsic structure of water in such solutions is meaningless. We believe that the best promise for understanding the structure of concentrated solutions is offered by the phenomenological model [2] whose underlying concept is that of correlation of the changes in the physicochemical properties of solution with the type of the solubility polytherm of the salt. Thereby, regions of existence in concentrated solutions of zones dominated by different structural units (cybotactic groups [3, 4] or hydrate forms) can be revealed. According to this concept, the structure of a cybotactic group corresponds to that of the solid phase [4] crystallizing from solution with decreasing temperature, specifically, to the structure of the crystal hydrate of a particular composition, or of the anhydrous salt.

Published data confirm the presence of cybotactic groups in concentrated solutions of inorganic salts of different nature. In [5], $Ni_2Cl_4 \cdot 12H_2O$ associates in a concentrated nickel chloride solution were detected and characterized using the neutron scattering technique. An NMR spectroscopic examination revealed a M_2Cl_2 microalloy in solutions of potassium, rubidium, and cesium chlorides [6]. For example, in cesium chloride solutions, starting from the concentration of 5 mol $(H_2O\ kg)^{-1}$ [in the pre-eutectic region, < 8 mol $(H_2O\ kg)^{-1}$], microalloys of such dimers appear. Examinations by the technique of X-ray scattering in solution and single-crystal X-ray diffraction analysis [4] showed that the structure and composition of cybotactic groups correspond to those of the solid phase which crystallizes from this solution with decreasing temperature and whose unit cell dimensions correspond to those of the crystal hydrate.

We explored the structure of aqueous electrolyte solutions based on the concept of structural changes occurring therein as the solution concentration is varied. In selecting salts for our study, we considered the nature of the salt (anhydrous, crystal hydrates), with the properties of positively and negatively hydrated cations and anions [7] and the features of the solubility polytherms of the salts [8] taken into account. Among the salts we chose, CsCl and $NaNO_3$ crystallize as anhydrous salts from concentrated aqueous solutions as temperature decreases, while LiCl, $LiNO_3$, $LiClO_4$, $NaClO_4$, and Na_2SO_4 crystallize in the form of crystal hydrates. In terms of crystallization branches in the solubility polytherms at temperatures up to 25°C, LiCl exhibits four crystallization branches ($LiCl{\cdot}5H_2O$, $LiCl{\cdot}3H_2O$, $LiCl{\cdot}2H_2O$, and $LiCl{\cdot}H_2O$) along with the water crystallization branch; $NaClO_4$ exhibits two crystallization branches ($NaClO_4{\cdot}2H_2O$ and $NaClO_4{\cdot}H_2O$), and $LiNO_3$, $LiClO_4$, and Na_2SO_4, one crystallization branch ($LiClO_4{\cdot}3H_2O$, $LiNO_3{\cdot}3H_2O$, and $Na_2SO_4{\cdot}10H_2O$, respectively). The reason for choosing NaCl was that its solubility polytherm is composed of two crystallization branches corresponding to sodium chloride dihydrate and anhydrous NaCl.

In this study, we used the near infrared (NIR) spectroscopic method. This choice was dictated by the fact that, using NIR spectra, it is possible to derive quantitative data for a large number of solutions over a wide concentration range, as required for application of chemometric analysis methods to the spectral data [9–14].

A number of studies were dedicated to examination of aqueous solutions of alkali metal salts by NIR and ATR spectroscopy [15, 16], followed by chemometric analysis [17–20]. In [17], five NIR spectra were measured at three temperatures for each of the aqueous solutions of NaCl, KCl, $MgCl_2$, and $AlCl_3$. The spectral data were processed by the Principal Component Analysis (PCA) and Multivariate Curve Resolution–Alternating Least Squares (MCR–ALS) methods. According to [17], in all the systems studied there exist three forms of water: strongly hydrogen-bonded water (its proportion tends to decrease with increasing temperature), weakly hydrogen-bonded water (its proportion tends to increase with increasing temperature), and an intermediate type of water. Another conclusion derived in [17] concerns differentiation of the salts based on how they affect the structure of pure water. Specifically, NaCl and KCl cause the hydrogen bond strength in water to decrease, while $MgCl_2$ and $AlCl_3$, to increase. In [18–20] it was found that over a wide concentration range in aqueous solutions of alkali metal halides there exist only two water types: pure water and water in hydrated salt. The factor analysis showed that the spectra of the aqueous salt solutions are linear combinations of those of pure water and the water of hydration. Both types of water are stable throughout the concentration range of existence of a homogeneous salt solution.

In [21], solvent-separated and contact ion pairs were discussed which, in our opinion, are part, or fragments, of hydrates of the salts studied, rather than individual structural units. Here we interpreted the results of analysis of the NIR spectroscopic data for aqueous solutions of different concentrations in terms of formation and conversion of hydrated forms of salts in solutions.

The IR spectra of the aqueous solutions of the salts in the frequency range of 7500–5400 cm^{-1} (Fig. 1) were processed by the PCA and MCR–ALS methods [14]. This frequency range contains bands of the O–H stretching vibrations of water, so the results of chemometric analysis reflect different states of the water molecules in the system.

The interpretation of the spectral data processed by the PCA and MCR–ALS methods is based on the assumption that the structure of the solution is identical to that of the solid phase crystallizing therefrom with decreasing temperature [4–6].

System $LiClO_4$–H_2O. Two spectral forms were found in this system using the PCA and MCR–ALS methods. As seen from Fig. 2, a correlation exists between the spectrum of the first form and that of pure water, and between the spectrum of the second form and that of the saturated solution. With increasing salt concentration in solution the proportion of the first spectral form tends to decrease, and that of the second spectral form, to increase up to saturation concentrations. The cryoscopic data (Fig. 3) and the single-crystal X-ray diffraction analysis data for lithium perchlorate trihydrate [22] indicate that, in the $LiClO_4$–H_2O system, the surrounding of the lithium ion remains unchanged with increasing salt concentration. Hence, throughout the concentration range of existence of a homogeneous solution, water is present in two forms. The first spectral form is pure water, and the second, water in the cybotactic group based on lithium perchlorate trihydrate, in which the Li^+ ion is surrounded by six water molecules.

System $LiNO_3$–H_2O. At a first glance, this system is identical to that of lithium perchlorate, since these

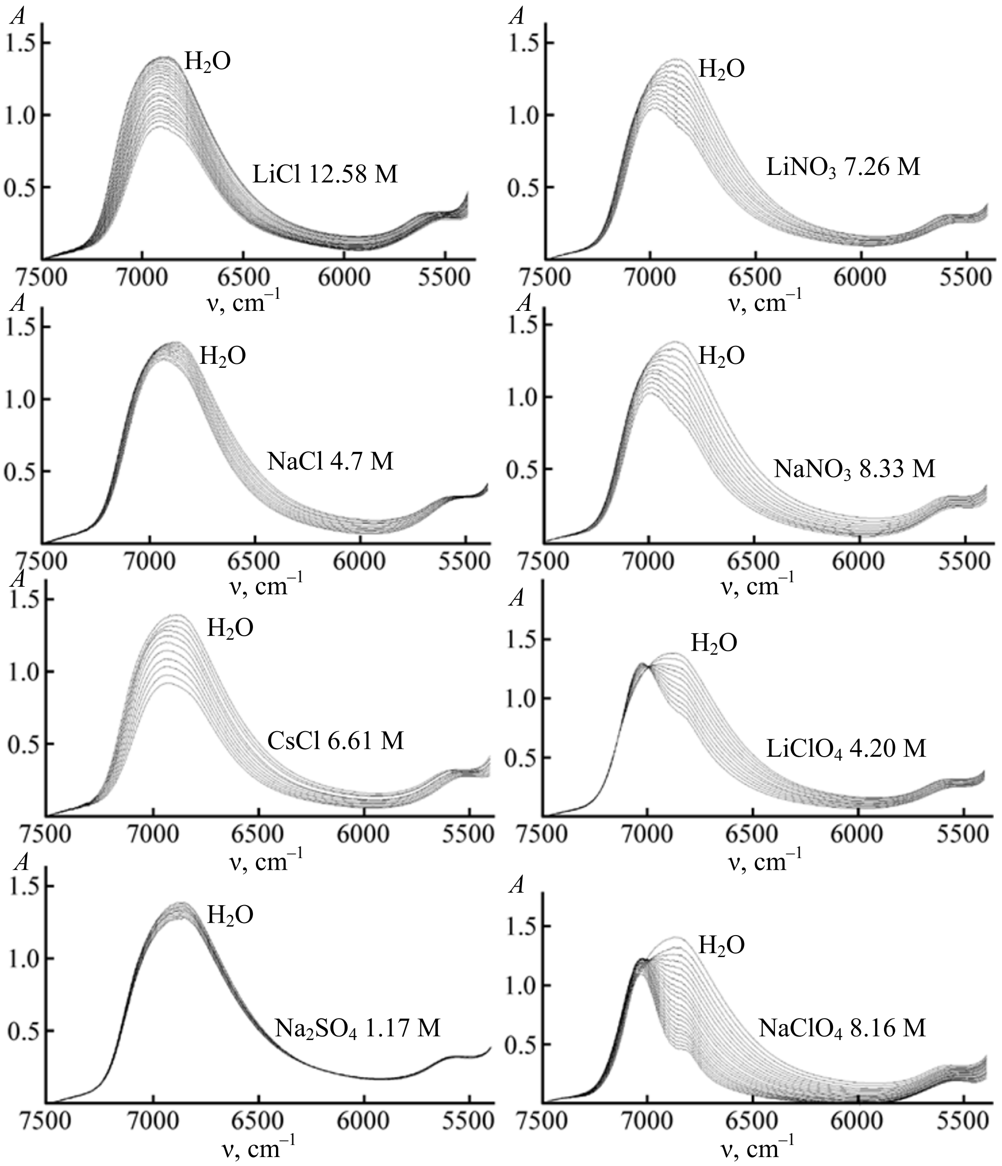

Fig. 1. IR spectra of water and aqueous solutions of the salts in the near IR region.

systems have solubility polytherms of similar shapes (Fig. 3) and form analogous crystal hydrates ($LiClO_4·3H_2O$, $LiNO_3·3H_2O$) crystallizing from the corresponding saturated solutions at 25°C. Spectral data processing by the PCA and MCR–ALS methods revealed two spectral forms of water (Fig. 2). According to the data of single-crystal X-ray diffraction analysis for $LiNO_3·3H_2O$ [23] the Li^+ ion in the first hydration shell is surrounded by four water molecules and two NO_3^- ions. Chemometric analysis of the spectral data revealed only two spectral forms which we believe to be pure water and water in the cybotactic group based on lithium nitrate trihydrate.

System $NaClO_4$–H_2O. According to the solubility polytherm of $NaClO_4$ (Fig. 3), the concentration range of the solution is subdivided into three regions dominated by the following structures: water, sodium perchlorate dihydrate, and sodium perchlorate monohydrate. The PCA and MCR–ALS analysis of the spectral data for the aqueous solutions of sodium perchlorate revealed the presence of three spectral forms of water (Fig. 2). Among them, one form corresponds to pure water, and its proportion tends to decrease with increasing salt concentration. The other two forms we interpreted on the basis of the cryoscopic and X-ray diffraction data for the salt hydrates.

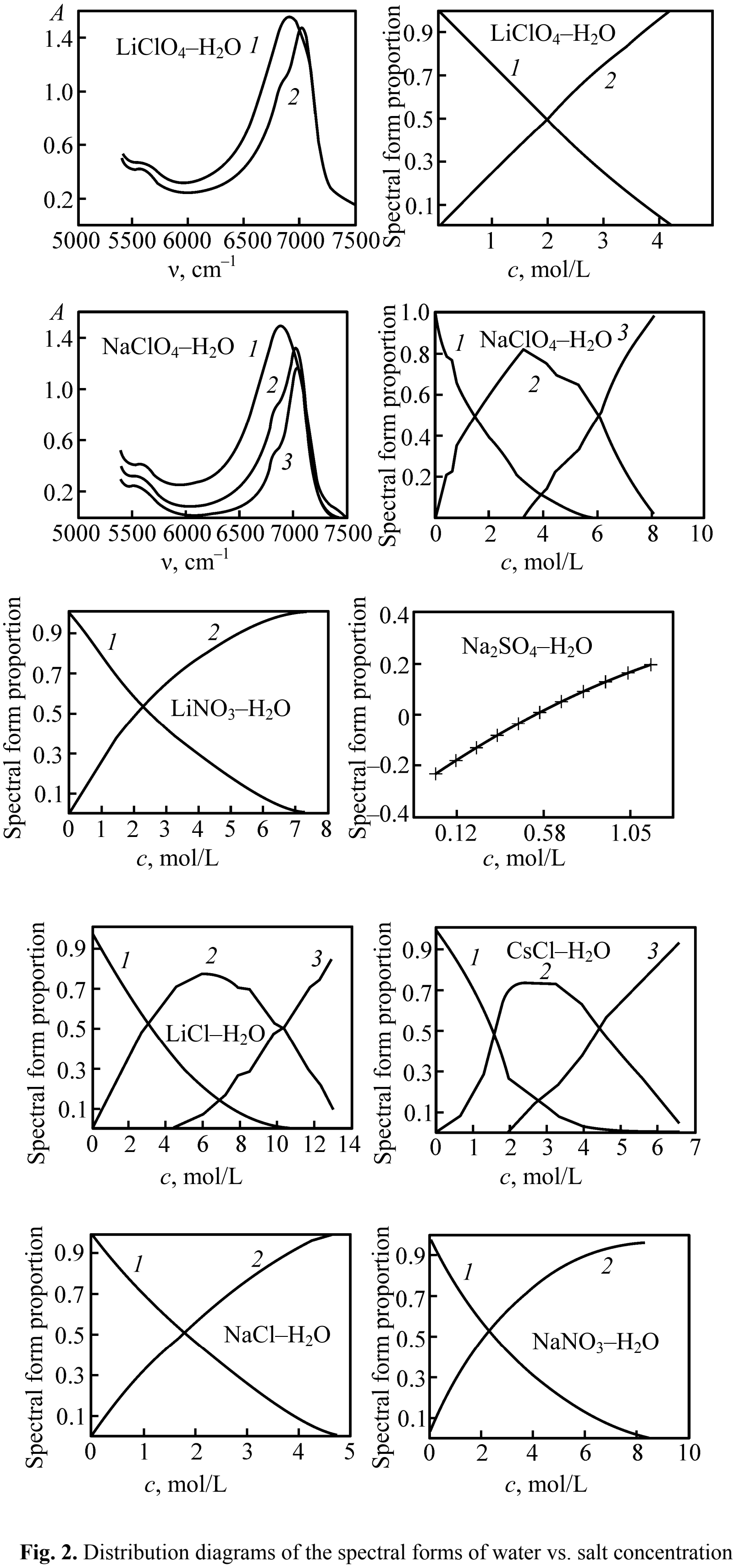

Fig. 2. Distribution diagrams of the spectral forms of water vs. salt concentration.

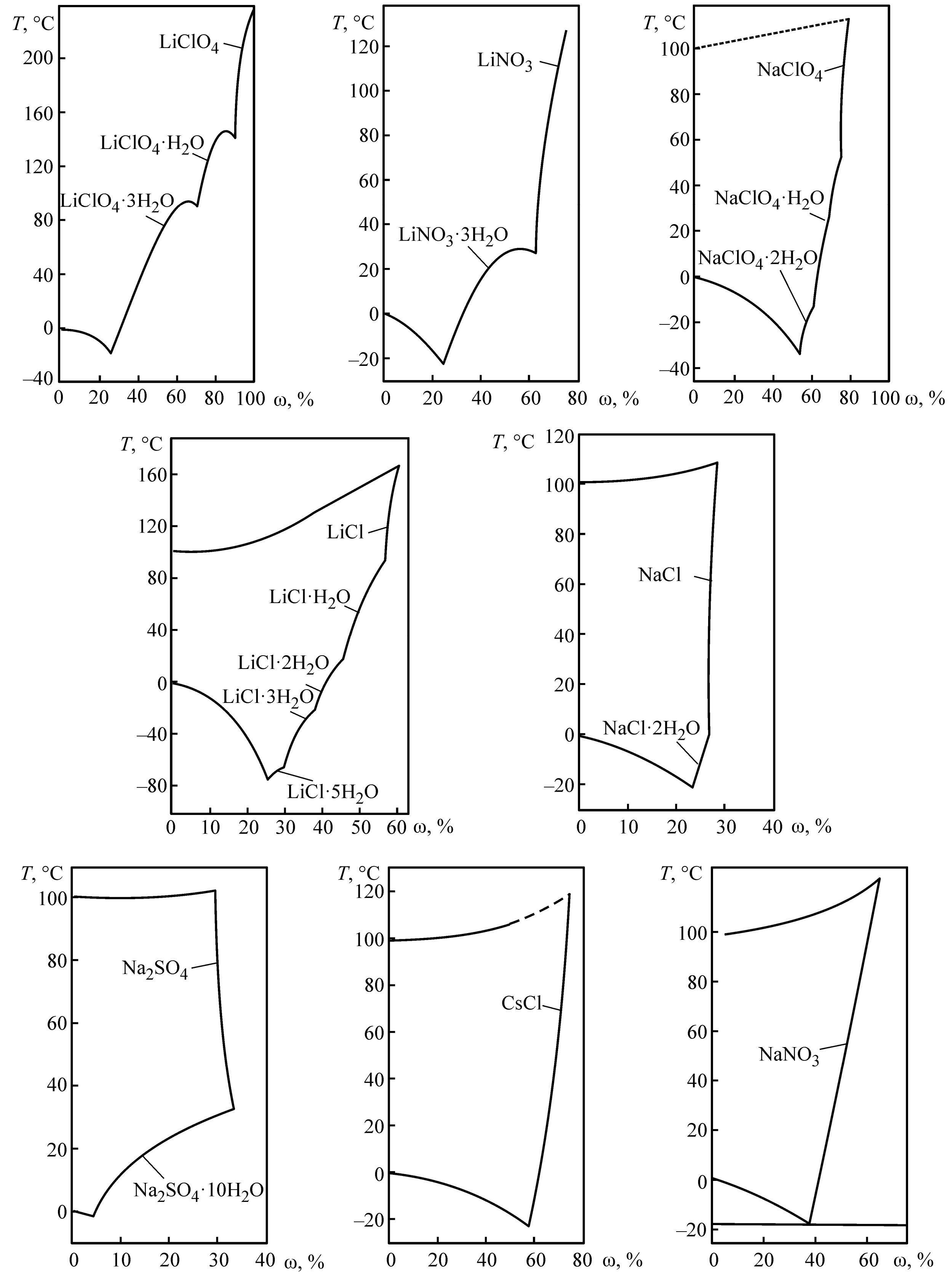

Fig. 3. Solubility polytherms of the salts studied.

As the salt concentration in solution increases, the proportion of the second spectral form initially increases and then decreases. The third spectral form appears at the concentration of ~3.2 M, and its proportion tends to increase up to saturation concentrations. From the saturated solution at room temperature sodium perchlorate monohydrate crystallizes. The X-ray diffraction analysis shows that in the crystal lattice the Na^+ ion is surrounded by two water molecules and four ClO_4^- ions [24]. We regard the second spectral form as corresponding to water in the cybotactic group based on sodium perchlorate dihydrate, in which six water molecules are bound to the sodium ion, and the third spectral form as water in the cybotactic group based on sodium perchlorate monohydrate, in which a part of the water molecules are replaced by the ClO_4^- ions in the first hydration shell of the cation.

System $LiCl–H_2O$. The solubility polytherm of LiCl (Fig. 3) at temperatures up to 25°C in the post-eutectic region exhibits four crystallization branches corresponding to $LiCl·5H_2O$, $LiCl·3H_2O$, $LiCl·2H_2O$, and $LiCl·H_2O$ hydrates, respectively. The PCA and MCR–ALS analysis of the spectral data for the aqueous LiCl solutions revealed three spectral forms of water (Fig. 2). The first spectral form correlates with the spectrum of pure water; its proportion tends to decrease with increasing salt concentration. As to the second spectral form, we interpreted it as water in the cybotactic group in which the cation is surrounded by six water molecules in the first hydration shell. With increasing salt concentration the proportion of this form initially increases and then decreases. The third spectral form appears at the salt concentration of ~4.5 M; its proportion tends to increase up to saturation concentrations. In our view, it corresponds to water contained in the $LiCl·H_2O$ cybotactic groups. The X-ray single-crystal diffraction analysis of $LiCl·H_2O$ [25] showed that the Li^+ ion is surrounded by two water molecules and four Cl^- ions. For $LiCl·5H_2O$, $LiCl·3H_2O$, and $LiCl·2H_2O$ crystal hydrates, no published X-ray diffraction data are available. Evidently, with changing solution concentration, the qualitative composition of the nearest surrounding of the Li^+ ion changes from six water molecules to two water molecules and four Cl^- ions. The second spectral form most likely belongs to water from the cybotactic group based on $LiCl·5H_2O$. As to participation of the $LiCl·3H_2O$ and $LiCl·2H_2O$ cybotactic groups in the formation of any spectral forms, this is a problem which requires further elucidation.

System $NaCl–H_2O$. The first spectral form in the MCR–ALS diagram for the $NaCl–H_2O$ system corresponds to pure water. To interpret the second form of water, we considered the solubility polytherm of NaCl (Fig. 3). With increasing salt concentration sodium chloride dihydrate and the anhydrous salt crystallize from the solution after the eutectic. Importantly, the concentration range in which the anhydrous NaCl salt crystallizes is very narrow; its crystallization branch in the solubility polytherm of the salt is nearly vertical. Therefore, the changes associated with formation of the anhydrous NaCl salt may be unobservable in the MCR–ALS diagram. The second spectral form belongs to water in the cybotactic group based on sodium chloride dihydrate in which, according to [26], two water molecules in the first hydration sphere of the cation are replaced by Cl^- ions.

System $Na_2SO_4–H_2O$. The solubility polytherm of Na_2SO_4 is shown in Fig. 3. There exists a very narrow range in which the water structure dominates, i.e., water is the solvent, and in which ice crystallizes from solution with decreasing temperature [0–4 mol %, 0–0.29 mol $(H_2O\ kg)^{-1}$]. In the $Na_2SO_4–H_2O$ system, $Na_2SO_4·10H_2O$ crystallizes from the saturated solution at 25°C. In terms of the phenomenological model of the structure of aqueous electrolyte solutions [2], in the post-eutectic region [$c > 0.29$ mol $(H_2O\ kg)^{-1}$], the structure of the solution is determined by that of sodium sulfate decahydrate. The PCA and MCR–ALS analysis of the spectral data for the aqueous Na_2SO_4 solutions revealed a sole principal component in the system (Table 1, Fig. 2). Presumably, this spectral form of water belongs to water in the cybotactic group based on sodium sulfate decahydrate, since with increasing salt concentration the proportion of the spectral form of water in the cybotactic group tends to increase, and that of the spectral form of pure water should tend to decrease. We believe that this system contains a pure water form, but its proportion is very small compared to that of water contained in the cybotactic groups based on sodium sulfate decahydrate.

System $CsCl–H_2O$. The characteristic features of the $CsCl–H_2O$ system include crystallization of the anhydrous salt from the saturated solution at 25°C (Fig. 3) and negative hydration of the Cs^+ ion [7]. For this system, three spectral forms of water were revealed by the PCA and MCR–ALS analysis (Fig. 2). Generally, two processes occur simultaneously when a salt is added to water: destruction of the intrinsic structure of water and hydration, i.e., structuring of the

Table 1. Results of analysis of the spectral data matrix for the Na_2SO_4–H_2O system by the PCA method

Principal component no.	Eigenvalue of the data matrix	Variability described by the principal component, %	Variability described by the sum of the principal components, %
1	6.25×10^{2}	99.996	99.996
2	2.02×10^{-2}	0.003	99.999
3	2.63×10^{-3}	0	100

Table 2. Characteristics of the aqueous solutions of the salts studied

Salt	Highest concentration in the series of solutions, M	Step of the initial solution diluting for spectral measurements, M	Number of crystallization branches in the solubility polytherm at temperatures up to 25°C	Number of the principal components in the system at 25°C	Number of cybotactic groups in solution at 25°C
$LiClO_4$	4.20	0.420	2	2	1
$LiNO_3$	7.26	0.726	2	2	1
$NaClO_4$	8.16	0.408	3	3	2
LiCl	12.98	0.649	5	3	4
NaCl	5.03	0.503	3	2	2
Na_2SO_4	1.17	0.117	2	1	1
CsCl	6.61	0.661	2	3	1
$NaNO_3$	8.33	0.833	2	2	1

water molecules around the ion. With positively hydrated ions, the latter process dominates and is manifested in the MCR–ALS diagrams (this is the case of all previously described systems). As to the Cs^+ ion, it is negatively hydrated, and the hydration process in the CsCl–H_2O system is weakly pronounced. Hence, water destruction is the dominant process observed in the diagrams. Thus, the first spectral form (Fig. 2) corresponds to pure structured water whose proportion in the system tends to decrease with increasing salt concentration because of cleavage of the hydrogen bonds between the water molecules. The second spectral form (Fig. 2) seems to belong to water that underwent destruction with cleavage of hydrogen bonds and possibly exists in the monomeric form. With increasing salt concentration its proportion initially tends to increase and then, to decrease (the proportion of water in the monomeric form increases as long as destruction of pure water occurs, and decreases when the water structuring process starts once again). The third spectral form (Fig. 2) appears at the concentration of 2 M; it belongs to water liberated during the formation of Cs–Cl contact ion pairs and structured once again with the formation of hydrogen bonds.

System $NaNO_3$–H_2O. From the saturated $NaNO_3$ solution at room temperature (25°C), like in the case of CsCl, the anhydrous salt crystallizes (Fig. 3), but the Na^+ ion is positively hydrated. The PCA and MCR–ALS analysis revealed two spectral forms of water in the $NaNO_3$–H_2O system (Fig. 2): pure water and water liberated during the formation of Na–NO_3 contact ion pairs.

To summarize the results obtained (Table 2), chemometric analysis of the spectral data, combined with application of the phenomenological model of the structure of aqueous electrolyte solutions, allows identifying water in essentially different states, specifically, pure water having its intrinsic structure and water contained in cybotactic groups. When several crystal hydrates of the salt are present, water transitions between cybotactic groups are observed.

Influence of the nature of the anion on the water structure in solution. The set of all the NIR spectra of the aqueous solutions studied (NaCl, LiCl, CsCl, $NaNO_3$, $LiNO_3$, $NaClO_4$, $LiClO_4$, and Na_2SO_4) was analyzed by the PCA method. Figure 4 presents the PCA scores plotted for the general matrix of the experimental IR spectra in the coordinates of the first and second principal components. Each point in the plot corresponds to the spectrum of one of the solutions studied. As seen from Fig. 4, the objects are grouped in mathematical clusters depending on the nature of the salt anion, which is manifested primarily

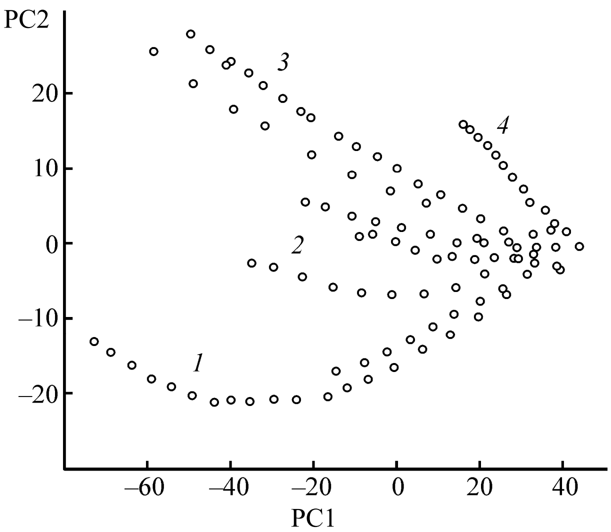

Fig. 4. PCA scores plot for the general matrix of the experimental IR spectra of the aqueous salt solutions in the PC1–PC2 coordinates. Digits indicate clusters of the IR spectra of the solutions of (*1*) lithium and sodium perchlorates, (*2*) lithium and sodium nitrates, (*3*) lithium, sodium, and cesium chlorides, and (*4*) sodium sulfate.

in the features of the anion–water interaction. The first cluster includes lithium and sodium perchlorates, the second cluster, lithium and sodium nitrates, the third cluster, lithium, sodium, and cesium chlorides, and the fourth cluster, sodium sulfate. The sequence of the clusters of the aqueous salt solutions (from bottom to top in the plot) is as follows: ClO_4^-, NO_3^-, Cl^-, SO_4^{2-} (Fig. 4).

In [27], the IR spectra of aqueous solutions of sodium salts were analyzed, and the positions of the absorption band maxima were determined for the stretching vibrations ν_{OD} of water (HDO) in the salt solutions studied. It was found that the strength of interaction between the anion and the coordinated water molecules increases as $ClO_4^- < NO_3^- < Cl^- < SO_4^{2-}$; the proton-acceptor power of the anions correlates with the surface charges. A conclusion was made that the ClO_4^-, NO_3^-, and Cl^- anions in aqueous solutions form weaker, and the SO_4^{2-} anion, stronger (compared to the average energy of the hydrogen bonds between the molecules in pure water) hydrogen bonds with the coordinated water molecules.

Table 3. Correlation of the distribution of the IR spectra of the aqueous electrolyte solutions in the PCA scores plot with the hydration enthalpy of the anion.

Type and sequence of anions in the PCA scores plot	Hydration enthalpy of the anion, kJ mol^{-1} [28]	Hydration enthalpy of the anion, kJ mol^{-1} [29]
ClO_4^-	–229	–200
NO_3^-	–314	–284
Cl^-	–381	–326
SO_4^{2-}	–1059	–

Table 3 lists the hydration enthalpies of the anions [28, 29]. In [28], the hydration enthalpy of the anion was calculated by the formula:

$$\Delta H^0_{\text{hyd}} = -700z^2/r.$$

Here *r*, Å, is the Pauling's crystal radius for Cl^- ion, and $r = r_t + 0.3$ for ClO_4^-, NO_3^-, and SO_4^{2-} ions, where r_t is the thermochemical radius.

In [29] the hydration enthalpies of the anions were determined under the assumption of equality between the hydration enthalpies of hydroxy and hydronium ions. Obviously, the PCA data correlate with the hydration enthalpies of the anions when treated as a relative measure of the strength of water bonding by the anions.

It should be noted that, inside each cluster, the sequence of systems is reproduced: first comes sodium salt, then lithium salt (from bottom to top in the plot). Hence, application of multivariate chemometric approach in analyzing broad unresolved bands in the NIR region of the spectra of the aqueous solutions has led to the differentiation of the objects under study depending not only on the nature of the anion but on the nature of the cation as well. In the PCA scores plot, the systems are ordered from bottom to top according to increasing strength of interaction of the ions with the water molecules, and the principle holds both for the anions [27] and cations [7].

Figure 5 presents the IR spectra of water and saturated aqueous solutions of the lithium and sodium salts. In the spectra of the aqueous solutions of the lithium salts, the shift of the absorption band maximum of water $\nu_{OH}(H_2O)$ to higher frequencies is the larger the weaker the anion–water interaction. The water–anion bond energy decreases as $Cl^- > NO_3^- > ClO_4^-$, and this is specifically responsible for a larger shift to higher frequencies (toward water with broken hydrogen bonds) of the absorption band maxima of the water bonded to these anions and for smaller overlapping of the bands of water and the anion-bonded water molecules. An analogous sequence is

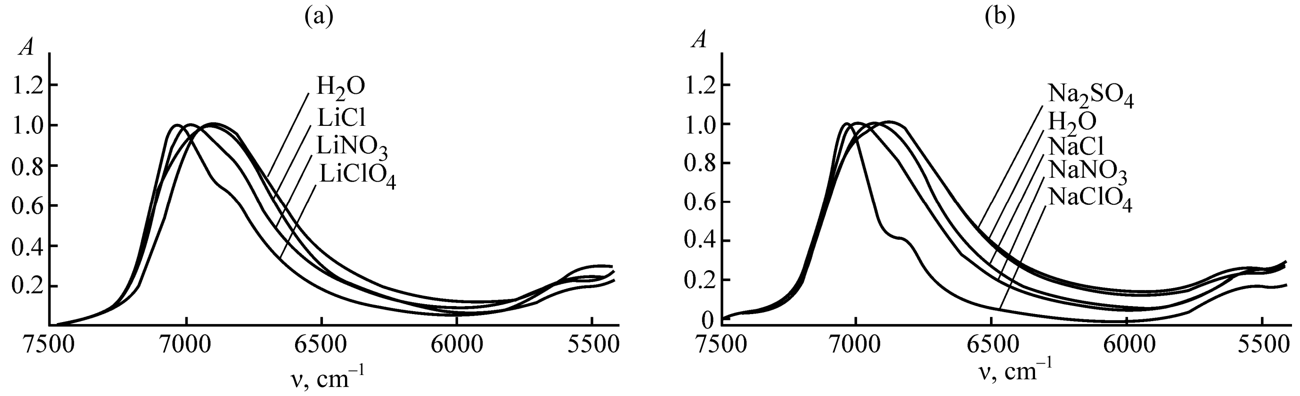

Fig. 5. IR spectra of water and concentrated aqueous solutions of the (a) lithium and (b) sodium salts.

observed for the positions of the maxima relative to those of pure water in the spectra of the aqueous solutions of the sodium salts: SO_4^{2-} >> H_2O > Cl^- > NO_3^- > ClO_4^-. These observations are consistent with the results of chemometric analysis of the spectral data for the aqueous solutions of the salts studied (Fig. 4) and also correlate with the conclusions made in [27].

As mentioned above, in the PCA scores plot for the general matrix of the experimental IR spectra, each point corresponds to the spectrum of one of the solutions with a particular concentration. Hence, the series of points in the individual branches correspond to the spectra of the systems over a wide concentration range. It is seen that the spectra of pure water and dilute solutions are compactly grouped on the right side of the diagram. With increasing salt concentration the spectra of the solutions exhibit ever stronger differences while shifting from right to left (Fig. 4). The plotted data show that in the salt solutions with pre-eutectic concentrations (in dilute solutions) the nature of the cation and the anion is scarcely manifested. From our viewpoint, the reason is the dominance of the water structure in this concentration region.

Influence of the nature of the cation on the water structure in solution. The influence of the nature of the cation on the water structure was discussed in detail in [30]. Here, we determined and compared the Δν versus salt concentration dependences for lithium, sodium, and cesium chloride solutions. To this end, the absorption band maxima of pure water and each solution in the series studied for these systems were determined. Next, the difference Δν between the frequencies of the absorption band maximum of ith solution and of that of pure water was estimated, and plots of Δν versus salt concentration in the lithium, sodium, and cesium chloride solutions were constructed. It is noteworthy that Li^+ and Na^+ are positively hydrated cations, and Cs^+ is a negatively hydrated cation.

In the plot (Fig. 6) there is a common concentration region for these aqueous solutions, in which the absorption band maximum of pure water is shifted to higher frequencies. In the spectra of the $LiCl–H_2O$ and $NaCl–H_2O$ systems, beyond the concentration of 3.5 M, no frequency shifts are observed up to saturation of the solution. As to the $CsCl–H_2O$ system, starting from the 4 M concentration, the absorption band maximum shifts toward that of pure water. We believe that this effect is due to the fact that during the formation of Cs–Cl contact ion pairs the anhydrous CsCl salt crystallizes from the solution with liberation of the molecules of hydration water, which form a polymeric structure via hydrogen bonding.

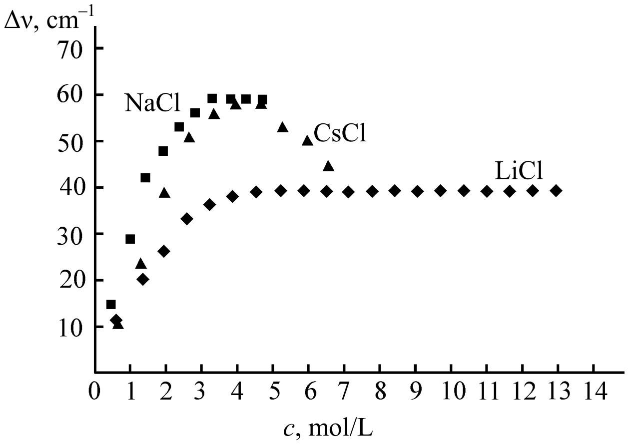

Fig. 6. Variation of Δν with the salt concentration in solution for lithium, sodium, and cesium chlorides.

Thus, we revealed a relationship between the number of the principal components and, correspondingly, the number of spectral forms of water in the system, on the one hand, and the number of the crystallization branches in the solubility polytherm of the salt, on the other. The number of spectral forms of water depends on whether the composition of the cybotactic group varies with changing salt concentration in solution. Regularity was detected in distribution of the IR spectra of the aqueous electrolyte solutions in the PCA scores plot depending on the character of interaction of the anion with the water molecules. The nature of the cation affects the solution structure depending on the type of hydration (positive or negative) of the cation and, consequently, on the type of the salt crystallization from the saturated solution at a particular temperature.

EXPERIMENTAL

The $LiClO_4$, $NaClO_4$, $LiNO_3$, $NaNO_3$, and LiCl salts used in this study were synthesized from the corresponding metal carbonates and appropriate acids and subsequently recrystallized twice from distilled water. Also, ultrapure NaCl, ultrapure CsCl, and chemically pure Na_2SO_4 were used; Na_2SO_4 before use was recrystallized twice. Solutions of these salts with the highest concentrations in the series were prepared by dissolving the corresponding salts in deionized water at 25°C. The concentration was determined by the gravimetric method. The analysis error was 0.5%. The salt solutions with lower salt concentrations were obtained by diluting the initial concentrated solutions using the gravimetric and volumetric methods. The concentrations of the initial solutions are listed in Table 2.

The IR spectra were recorded on a Spectrum BX Perkin Elmer spectrometer at 25°C in the first overtone of water at 5400–7500 cm^{-1} with the step 2 cm^{-1}; for the concentration step of the initial solution diluting, see Table 2. The solutions were prepared immediately before recording the spectra. The solution to be examined was placed in a glass cell with a 0.1-cm path length; number of scans was 50.

For each system studied, the experimental data matrix $A_{\text{exp}}(N_w,N_s)$, where N_w is the number of wavelengths, and N_s, number of measured spectra, was composed. For data processing by the principal component analysis method, the general matrix was constructed by combining all the matrices.

REFERENCES

1. Frank, H.S. and Wen, W.-Y., *Disc. Faraday Soc.*, 1957, vol. 24, p. 133.
2. Lilich, L.S. and Khripun, M.K., *Rastvory kak khimicheskie sistemy. Donorno-aktseptornye reaktsii v rastvorakh* (Solutions as Chemical Systems: Donor-Acceptor Reactions in Solutions), St. Petersburg: Sankt-Peterb. Gos. Univ., 2010.
3. Stewart, G.H., *Ind. J. Phys.*, 1932, vol. 7, no. 5, p. 603.
4. Davidian, A.G, Pestova, O.N., Starova, G.L., Gurzhii, V.V., Myund, L.A., and Khripun, M.K., *Russ. J. Gen. Chem.*, 2012, vol. 82, no. 4, p. 621. DOI: 10.1134/S1070363212040019.
5. Neilson, G.W. and Enderby, J.E., *Proc. R. Soc. London, Ser. A*, 1983, vol. 390, no. 1799, p. 353.
6. Hertz, H.G. and Mazitov, R., *Ber. Bunsen. Phys. Chem.*, 1981, vol. 85, no. 12, p. 1103.
7. Samoilov, O.Ya., *Struktura vodnykh rastvorov elektrolitov i gidratatsiya ionov* (The Structure of Aqueous Solutions of Electrolytes and Ion Hydration), Moscow: Akad. Nauk SSSR, 1957.
8. Kirgintsev, A.N., Trushnikova, L.N., and Lavrent'eva, V.G., *Rastvorimost' neorganicheskikh veshchestv v vode* (Solubility of Inorganic Substances in Water), Leningrad: Khimiya, 1972.
9. Kudrev, A.G., *Koord. Khim.*, 1999, vol. 25, no. 2, p. 152.
10. Kudrev, A.G., *Zh. Neorg. Khim.*, 2001, vol. 46, no. 5, p. 854
11. Kudrev, A.G., *Polym. Sci., Ser. A*, 2000, vol. 42, p. 527.
12. Gargallo, R., Eritja, R., and Kudrev, A.G., *Russ. J. Gen. Chem.*, 2010, vol. 80, no. 3, p. 485. DOI: 10.1134/S1070363210030205.
13. Bucek, P., Gargallo, R., and Kudrev, A.G., *Anal. Chim. Acta*, 2010, vol. 683, p. 69. DOI: 10.1016/j.aca.2010.10.008.
14. Davidian, A.G., Kudrev, A.G., Myund, L.A., and Khripun, M.K., *Russ. J. Gen. Chem.*, 2013, vol. 83, no. 3, p. 415. DOI: 10.1134/S107036321303002X.
15. Subramanian, S. and Fisher, H.F., *J. Chem. Phys.*, 1972, vol. 76, no. 1, p. 84. DOI: 10.1021/j100645a015.
16. Chen, Y., Zhang, Y.H., and Zhao, L.J., *Phys. Chem. Chem. Phys.*, 2004, vol. 6, p. 537. DOI: 10.1039/b311768e.
17. Gowen, A.A., Amigo, J.M., and Tsenkova, R., *Anal. Chim. Acta*, 2013, vol. 759, p. 8. DOI: 10.1016/j.aca.2012.10.007.
18. Max, J.J., De Blois, S., Veilleux, A., and Chapados, C., *Can. J. Chem.,* 2001, vol. 79, p. 13. DOI: 10.1139/cjc-79-1-13.
19. Max, J.J. and Chapados, C., *J. Chem. Phys.*, 2000, vol. 113, no. 16, p. 6803. DOI: 10.1063/1.1290133.

20. Max, J.J. and Chapados, C., *J. Chem. Phys.*, 2001, vol. 115, no. 6, p. 2664. DOI: 10.1063/1.1337047.
21. James, D.W. and Armishaw, R.F., *Aust. J. Chem.*, 1975, vol. 28, p. 1179.
22. Chomnilpan, S., Liminga, R., and Tellgren, R., *Acta Crystallogr., Sect. B*, 1977, vol. 33, p. 3954. DOI: 10.1107/S0567740877012588.
23. Hermansson, K., Thomas, J.O., and Olovsson, I., *Acta Crystallogr., Sect. B*, 1977, vol. 33, p. 2857.
24. Berglund, B., Tomas, J.O., and Tellgren, R., *Acta Crystallogr., Sect. B*, 1975, vol. 31, p. 1842. DOI: 10.1107/S0567740875006346.
25. Lerner, H.W. and Bolte, M., *Acta Crystallogr., Sect. E*, 2003, vol. 53, p. 20.
26. Klewe, B. and Pedersen, B., *Acta Crystallogr., Sect. B*, 1974, vol. 30, p. 2363.
27. Kristiansson, O., *Acta Univ. Upsaliensis*, 1989, p. 1.
28. Smith, D.W., *J. Chem. Educ.*, 1977, vol. 54, no. 9, p. 540. DOI: 10.1021/ed054p540.
29. Latysheva, V.A., *Vestn. Sankt-Petersb. Gos. Univ., Ser. 4*, 1998, issue 4 (no. 25), p. 99.
30. Davidian, A.G., Kudrev, A.G., Myund, L.A., and Khripun M.K., *J. Near Infrared Spectr.*, 2014, vol. 22, p. 27. DOI: 10.1255/jnirs.1090.